SUPPLEMENTARY INFORMATION
Polarized neutron diffraction using novel high Tc superconducting magnet on single crystal diffractometer POLI at MLZ

H. Thoma,[a,b]* W. Luberstetter,[a,b] J. Peters[c] and V. Hutanu [a,b]*

[a]*Institut für Kristallographie RWTH Aachen, Jägerstr. 17-19, 52056 Aachen, Germany,* [b]*Jülich Centre for Neutron Science JCNS at MLZ, Lichtenbergstr. 1, 85748 Garching, Germany, and* [c]*Forschungs-Neutronenquelle Heinz Maier-Leibnitz (FRM II), Lichtenbergstr. 1, 85748 Garching, Germany.*

E-mail: henrik.thoma@frm2.tum.de, vladimir.hutanu@frm2.tum.de

1. Technical/Practical use of the new HTS magnet

The outside dimensions of the HTS magnet are $596 \times 794 \times 363\,\mathrm{mm}^3$ (W × H × D), thus a rather compact design. The magnet weights 186 kg and is therefore significantly lighter than a classical electromagnet of the same field strength. Made from high Tc material, the superconducting coil packs are cooled cryogen-liquid free using a Gifford-McMahon type RDK-415D refrigerator, driven by an associated water-cooled He compressor type Sumitomo F-70H. The working temperature of the coils is between 15 K and 17 K. The cool down time for the magnet from room temperature to the ready for energization state is about 22.5 h, which is comparable to a typical value for a liquid He magnet and significantly faster than for other known 'dry' magnets used for neutron scattering (MLZ Magnets, 2017). Besides the easy and comfortable operation, the

magnet requires no maintenance for cryogen refilling and has no costs for cryo-fluids. Using the 'dry' cold head for cooling permits turning of the whole magnet in order to produce both vertical and horizontal field configurations by request. The magnet is powered by two Kepco BOP 6-125 power supplies, operating at a current of 208 A for the maximal field of 2.2 T. This maximal field can be reached with a fast ramping time of 6 min. Variable field ramping rates are also available for in-situ studies. A field homogeneity of 1.45% over the central sphere at the sample location with 15 mm diameter is guaranteed. The absolute field value is increasing while moving from the center of the split coil gap toward the coil body along the z-axis (blue continuous line in Fig. 1b in the main text). Taking into account the 80 mm large split gap in the magnet, it is possible to reach fields up to 2.5 T for small samples by placing them above/below the equatorial plane. By fixing the magnet on POLI with its equatorial field plane 20 mm above the beam plane, the full advantage of the available detector lifting mechanics on POLI (nu angle of totally 35°) can be reached. In order to reach nearly the maximal available in-plane scattering angle (gamma 130°) on POLI, the magnet can be fixed in a way that the incoming beam enters the magnet by an angle of about $-20°$ in regard to the x-axis shown in Fig. 1a in the main text.

2. Development of the guide field segment

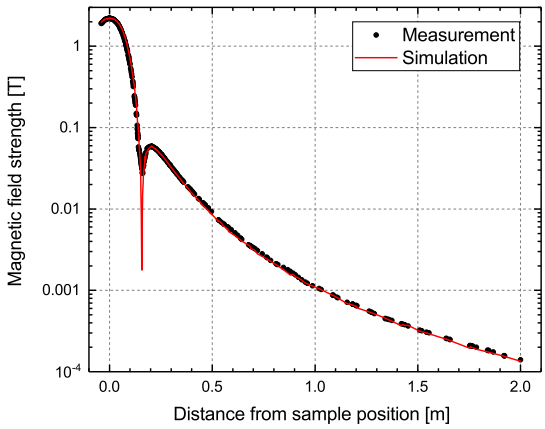

Fig. S1. Distribution of the magnetic field strength along the x-axis at the maximal field of $2.2\,T$ in the magnet. For axis convention see Fig. 1a in the main text. The continuous line shows the simulated values from our numerical COMSOL Multiphysics® model. The filled symbols represent the measured data provided by HTS-110 Inc. The figure shows, that our digital model, used for further optimization of the whole setup, describes almost perfectly the magnetic behaviour inside and outside the magnet.

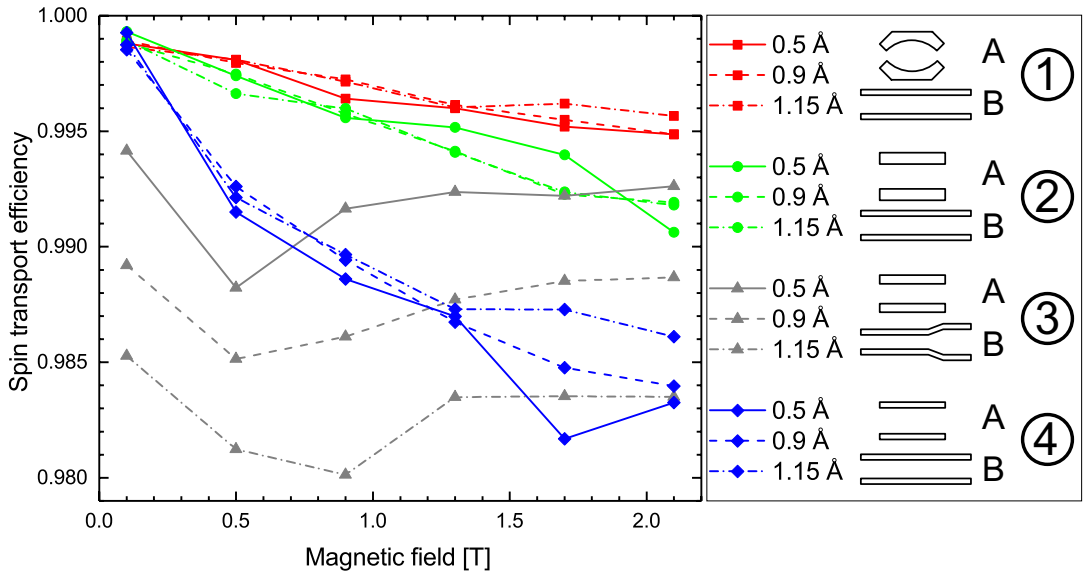

Fig. S2. Polarized neutron spin transport efficiency P_t as function of the main field in the magnet, calculated for different geometries of the guide field's pole pieces and for typical wavelengths on POLI. The A view shows the cross section of the pole pieces in the plane normal to the beam. The B view shows the shape along the beam. Cases two and four differ only in their thickness, whereas case one uses curved poles with optimised shape and case three has an inclined part along the beam direction to reduce the influence of the stray fields. Case two, showing a negligible small reduction of the efficiency at higher fields, however being much easier and cheaper in the production, has been used in the final design.

3. Development of the Mezei type spin flipper

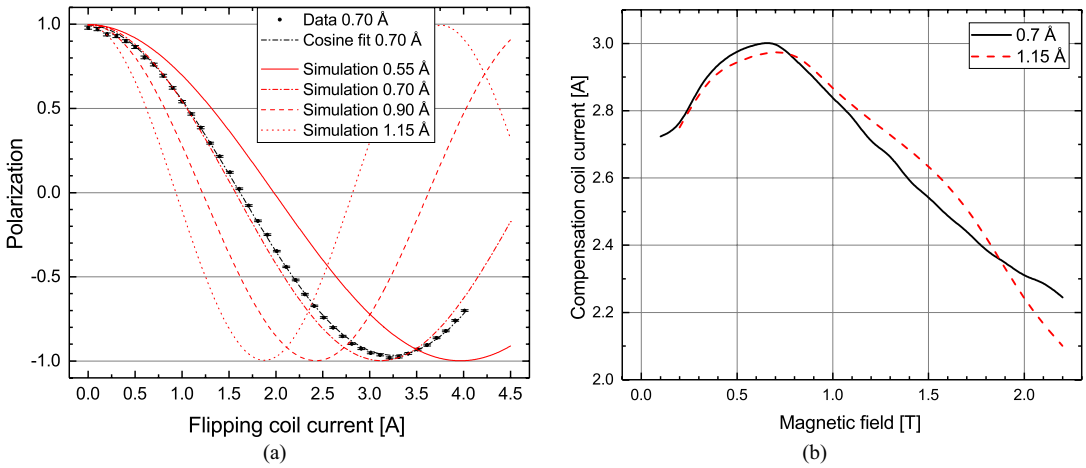

Fig. S3. (a) Neutron polarization as function of the current in the flipping coil of the Mezei flipper, while applying the optimal current in the correction coil. The lines represent the ideal values, calculated for different wavelengths used on POLI. The filled symbols represent the measured polarization normalised for the efficiency of polarizer and analyzer, respectively, with 0.7 Å wavelength and a sample field of 1.0 T. The curve between the symbols is a cosine fit to the data, showing a very good agreement to the calculated values and an almost perfect flipping efficiency. (b) Current in the correction coil of the flipper as function of the main field in the magnet, calibrated for neutron wavelengths of 0.7 Å and 1.15 Å.

In order to provide an efficient 180° spin flip for short wavelength neutrons (e.g. 0.55 Å used on POLI) a field integral of about 123 Oe cm must be provided inside the flipping coil. To produce a homogeneous field, required for a good flipping efficiency over the complete beam cross section, a height of 130 mm and a width of 140 mm was adopted for the rectangular coils. Anodized Al wires of 1 mm diameter were used for the windings. Using COMSOL Multiphysics®, it is possible to simulate multiple physical properties, like in our case not only the field integral from the applied current in the rectangular coils, but also the Joule heat produced by the current in the coils. The result of these simulations regarding heat dissipation were validated with an existing flipper made of similar wires. It was shown, that by the passive convection

in the ambient air, currents of maximal 2.5 A can be used for long time operation, because of the heating. Using an active convection cooling by pressure air blowing on the same coil, currents up to 4.5 A can be securely applied. Using 4 A as a targeted working current value for the shortest wavelength and the real coil geometry (number of windings, wire cross section, etc.) the length of the flipper coil in the beam was fixed to 26 mm. The new coils were provided with adjustable air flow from the existing pressure air supply network at the instrument. The requested current for a spin turn using this coil was simulated for different wavelengths used on POLI. The results are shown as red curves in Fig. S3a. The measured values for a wavelength of 0.7 Å are also shown in the same figure for comparison. With only a minimal shift of 0.1 A toward higher currents between the simulated values from our digital model and the real device on the instrument, this could be considered as a rather good agreement. The measured calibration curve is perfectly fitted with a cosine function. The flipping current values depend only on the energy of the neutron and should be independent of the field in the magnet. To decouple the main and the flipper field, the distance between flipper and magnet is usually increased. Since this is not possible due to the limited space at POLI, a separate guide field for the Mezei flipper (pos. 5 in Fig. 3a in the main text) was developed and simulated. To cover the complete beam cross section of about 40 mm in diameter with a homogeneous magnetic field of about 40 Oe, permanent NdFeB magnets (small yellow parts in pos. 5 in Fig. 3a) and inclined pole pieces for guiding (in orange) are added, leading to a stable and independent flipping coil environment. To reduce the influence of the HTS magnet's fringe field on the guide field in the flipper, the whole flipper is shielded by a 5 mm thick iron casing (dark gray in Fig. 3a, pos. 5). To compensate for variation of the guide and fringe field in the magnet, the flipper's compensation coil is used. In the described setup, the guide field is an extracted part of the magnet's main field. As a consequence, the strength of the

guide field will directly depend on the magnitude of the main field in the magnet, and therefore influence also the guide field's strength at the flipper. Fig. S3b shows the calibration curves for the current in the compensation coil as function of the main field in the magnet for two different wavelengths. The compensation current is wavelength independent and reaches a maximum at about 0.7 T in the magnet. Afterwards, the current decrease is almost linear with the field. This is easy to understand by taking into account, that the fringe field of the magnet also increases proportional to the main field and supports the compensation of the constant guide field in flipper. A flipping efficiency higher than 99% was experimentally proven for different wavelengths and all fields in the HTS magnet.

References

MLZ Magnets, (2017).
URL: *http://mlz-garching.de/englisch/instruments-und-labs/sample-environment/magnetic-fields.html*